

Interner Bericht

Efficient Bidirectional Path Tracing by Randomized Quasi-Monte Carlo Integration

T. Kollig, A. Keller

310/01



Efficient Bidirectional Path Tracing by Randomized Quasi-Monte Carlo Integration

T. Kollig, A. Keller

310/01

Universität Kaiserslautern
AG Numerische Algorithmen
Postfach 30 49
67653 Kaiserslautern
Germany

März 2001

Herausgeber: AG Numerische Algorithmen
Leiter: Professor Dr. S. Heinrich

Efficient Bidirectional Path Tracing by Randomized Quasi-Monte Carlo Integration

Thomas Kollig and Alexander Keller

Kaiserslautern University, 67653 Kaiserslautern, Germany

Abstract. As opposed to Monte Carlo integration the quasi-Monte Carlo method does not allow for an (consistent) error estimate from the samples used for the integral approximation. In addition the deterministic error bound of quasi-Monte Carlo integration is not accessible in the setting of computer graphics, since usually the integrands are of unbounded variation. The structure of the high dimensional functionals to be computed for photorealistic image synthesis implies the application of the randomized quasi-Monte Carlo method. Thus we can exploit low discrepancy sampling and at the same time we can estimate the variance. The resulting technique is much more efficient than previous bidirectional path tracing algorithms.

1 Introduction

The global illumination problem consists in rendering a photorealistic image of a virtual scene and camera description. A very basic algorithm for the solution of this light transport problem is the bidirectional path tracing algorithm [LW93, VG94], which in the context of the quasi-Monte Carlo method has been investigated in [Kel98b]. We generalize this work by introducing multiple importance sampling for the quasi-Monte Carlo method.

Numerical experiments show that the deterministic quasi-Monte Carlo method is superior to random sampling, but no (consistent) error estimate is available for the deterministic method. However, an error estimate would allow for adaptive sampling making the rendering much more efficient. Using randomized quasi-Monte Carlo the variance and thus the error can be estimated by sacrificing only a little bit performance. By numerical experiments we analyze different randomized quasi-Monte Carlo approaches and illustrate how they smoothly blend between the pure Monte Carlo and the quasi-Monte Carlo case.

2 Bidirectional Path Tracing

We briefly recall the global illumination problem and its path integral formulation. Applied to that formulation multiple importance sampling yields the bidirectional path tracing algorithm. Furthermore we address the problem of insufficient techniques that is inherent with multiple importance sampling.

2.1 The Global Illumination Problem

The light transport in vacuum is governed by a second kind Fredholm integral equation. By

$$L(y \rightarrow z) = L_e(y \rightarrow z) + \int_S L(x \rightarrow y) f_s(x \rightarrow y \rightarrow z) G(x \leftrightarrow y) dA(x) \quad (1)$$

we denote the radiance leaving a point $y \in S$ towards the point $z \in S$, where S is the boundary of the scene geometry. Light sources are defined by their emittance L_e . The bidirectional scattering distribution function f_s describes the surface properties. A is the area measure and

$$G(x \leftrightarrow y) := V(x \leftrightarrow y) \frac{|\cos \theta_x| |\cos \theta_y|}{|x - y|^2}$$

the geometry term, where θ_x is the angle between the surface normal in x and the vector between x and y , θ_y is defined analogously, and the visibility function is

$$V(x \leftrightarrow y) := \begin{cases} 1 & \text{if } x \text{ and } y \text{ are mutually visible} \\ 0 & \text{else} \end{cases}$$

The global illumination problem consists in computing functionals

$$I_j = \int_{S \times S} W_e^{(j)}(x \rightarrow y) L(x \rightarrow y) G(x \leftrightarrow y) dA(y) dA(x) \quad (2)$$

of the solution of the above integral equation for given detector functionals $W_e^{(j)}$, which formalize the camera description.

2.2 Path Integral Formulation of the Global Illumination Problem

A light path \bar{x} is characterized by its interaction points x_i with the scene surface S . The path space

$$\mathcal{P} := \bigcup_{k=1}^{\infty} \mathcal{P}_k$$

is the union of all path spaces

$$\mathcal{P}_k := \{\bar{x} = x_0 x_1 \dots x_k \mid x_i \in S \text{ for } 0 \leq i \leq k\} .$$

of a specific light path length k . For $D_0, D_1, \dots, D_k \subseteq S$ we define the measure

$$\mu_k(D_0 \times D_1 \times \dots \times D_k) := A(D_0) \cdot A(D_1) \cdot \dots \cdot A(D_k)$$

and

$$\mu(D) := \sum_{k=1}^{\infty} \mu_k(D \cap \mathcal{P}_k)$$

for $D \subseteq \mathcal{P}$. For a path $\bar{x} = x_0 x_1 \dots x_k \in \mathcal{P}_k$ the measurement contribution function is defined as

$$f_j(\bar{x}) := L_e(x_0 \rightarrow x_1)G(x_0 \leftrightarrow x_1) \cdot \left(\prod_{i=1}^{k-1} f_s(x_{i-1} \rightarrow x_i \rightarrow x_{i+1})G(x_i \leftrightarrow x_{i+1}) \right) \cdot W_e^{(j)}(x_{k-1} \rightarrow x_k) .$$

If we recursively substitute L in the measurement equation (2) by the radiance integral equation (1), we get the Neumann series, which now can be formulated as path integral

$$I_j = \sum_{k=1}^{\infty} \int_{\mathcal{P}_k} f_j(\bar{x}) d\mu_k(\bar{x}) = \int_{\mathcal{P}} f_j(\bar{x}) d\mu(\bar{x}) . \quad (3)$$

2.3 Multiple Importance Sampling

Using the variance reduction technique of importance sampling [Sob94,KW86] the integral of f over a domain D can be estimated by

$$\int_D f(x) dx \approx \frac{1}{n} \sum_{i=1}^n \frac{f(\xi_i)}{p(\xi_i)} , \quad (4)$$

where p is a probability density function with $\text{supp } f \subseteq \text{supp } p$ and ξ_i are independent realizations of p -distributed random variables. The variance of the estimator in (4) depends on f and the choice of p .

Often it is possible to specify a whole set p_1, p_2, \dots, p_N of probability density functions instead of just a single p . While each probability density function of the set may reduce the variance of the estimator in (4) only in a possibly unknown subdomain of D , multiple importance sampling, a technique introduced by [VG94] and analyzed in [OZ99], allows to combine samples which are distributed according to different probability density functions and to reduce the variance.

A probability density function p can be used as a *technique*, if we are able to generate p -distributed samples and to evaluate $p(x)$ for a given $x \in D^1$. Assuming we have N techniques with their associated probability density functions

$$p_1, p_2, \dots, p_N : D \rightarrow \mathbb{R}_0^+ ,$$

a so called *heuristic* consists of N weight functions

$$w_1, w_2, \dots, w_N : D \rightarrow \mathbb{R}_0^+ ,$$

such that

¹ At least we must be able to decide whether $x \in \text{supp } p$ holds for a given $x \in D$.

- $\sum_{i=1}^N w_i(x) = 1$ for all $x \in D$ with $f(x) \neq 0$ and
- $w_i(x) = 0$ for all $x \in D$ with $p_i(x) = 0$

holds. Note that these conditions imply that for each $x \in \text{supp } f$ only at least one technique i has to exist with $x \in \text{supp } p_i$. Then the multiple importance sampling estimator

$$\int_D f(x) dx \approx \frac{1}{n} \sum_{j=1}^n \sum_{i=1}^N w_i(x_{i,j}) \frac{f(x_{i,j})}{p_i(x_{i,j})} \quad (5)$$

is unbiased, where the $x_{i,j}$ are p_i -distributed for $1 \leq i \leq N$ and $1 \leq j \leq n$.

Example: The balance heuristic has the weight functions

$$w_i(x) := \frac{p_i(x)}{\sum_{\ell=1}^N p_\ell(x)} \quad (6)$$

for $1 \leq i \leq N$. Inserting these into (5) yields

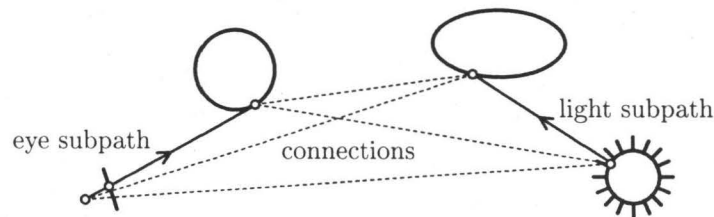
$$\int_D f(x) dx \approx \frac{1}{n} \sum_{j=1}^n \sum_{i=1}^N \frac{f(x_{i,j})}{\sum_{\ell=1}^N p_\ell(x_{i,j})}.$$

The behaviour of a multiple importance sampling estimator using balance heuristic is comparable to the importance sampling estimator with $p \equiv \frac{1}{N} \sum_{\ell=1}^N p_\ell$.

2.4 The Bidirectional Path Tracing Algorithm

Solving the global illumination problem using multiple importance sampling yields the bidirectional path tracing algorithm. The path space samples are generated in three steps:

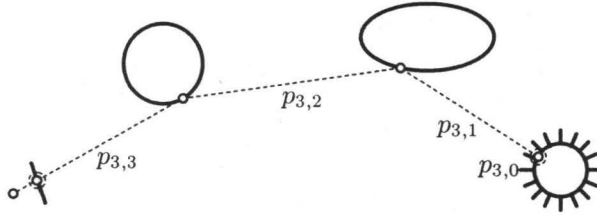
1. generate a light subpath,
2. generate an eye subpath, and
3. connect both subpaths deterministically.



In order to generate a light subpath a random point on a light source is chosen. Then a ray is shot into a random direction. The subsequent intersection point with the scene surface S is the next point of our subpath and so on. In the

same way an eye subpath is generated by starting a random walk from the eye point². Finally a light path $\bar{x} \in \mathcal{P}$ is obtained by connecting the endpoints of both subpaths. Since the ray casting function is very expensive, we use all possible connections as additional path space samples as illustrated in the figure above.

The resulting associated probability density functions are denoted by $p_{k,i}$, where k is the path length and i the number of points of the light subpath used to generate path space samples. The figure below shows all possible techniques with their associated probability density functions for path length $k = 3$, where each $p_{3,i}$ is positioned at its deterministic connection.



Applying multiple importance sampling (5) with the balance heuristic (6) to the global illumination problem (3) yields the bidirectional path tracing estimator

$$\sum_{k=1}^{\infty} \int_{\mathcal{P}_k} f_j(\bar{x}) d\mu_k(\bar{x}) \approx \sum_{k=1}^{\infty} \frac{1}{n} \sum_{j=1}^n \sum_{i=0}^k \frac{f_j(\bar{x}_{k,i,j})}{\sum_{\ell=0}^k p_{k,\ell}(\bar{x}_{k,i,j})}, \quad (7)$$

where n is the number of samples per technique and for $1 \leq j \leq n$ the $\bar{x}_{k,i,j}$ are generated according to $p_{k,i}$. In order to handle the infinite sum we can use absorbing Markov chains for subpath generation. A biased alternative is to compute the approximation up to a maximum path length k_{\max} .

The possibility to achieve a valid path using the *eye connection techniques* $p_{k,k}$, where the end of a light subpath is connected with the eye point, is very small and most samples are of zero contribution, if the image is computed pixel by pixel. Therefore we allow samples of these techniques to contribute directly to any pixel of the image.

2.5 The Problem of Insufficient Techniques

Multiple importance sampling tries to hide the weaknesses of single probability density functions, but nevertheless can fail. In order to illustrate the limits of the estimator (5) suppose we have a subdomain $G \subseteq D$ for which only one technique is accessible. Then multiple importance sampling degenerates to standard importance sampling (4) on G due to an insufficient set of techniques.

² Here we are using the simple pinhole camera model.

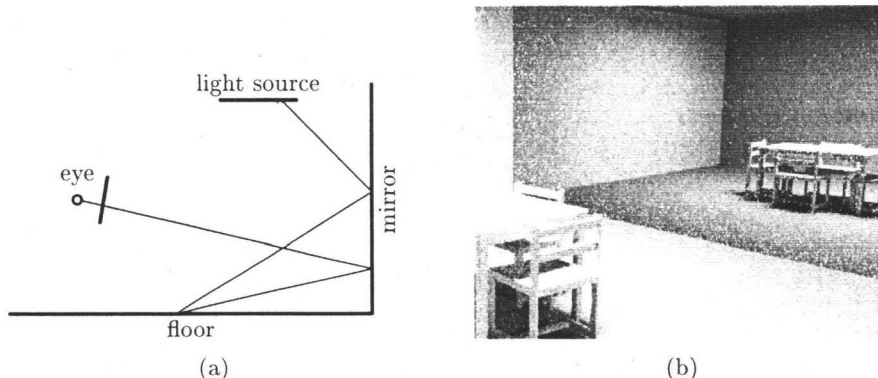


Fig. 1. The problem of insufficient techniques: (a) draft of difficult path and (b) resulting high variance.

For bidirectional path tracing the problem of insufficient techniques arises for singular surface properties, e.g. mirrors that usually are modeled by a Dirac delta distribution in the bidirectional scattering distribution function f_s . In Fig. 1 (a) such a difficult path is sketched: It can only be generated by one technique that uses no light subpath. The resulting high variance is clearly visible in Fig. 1 (b) and is perceived as white dots.

3 Quasi-Monte Carlo Bidirectional Path Tracing

The Koksma-Hlawka inequality predicts that quasi-Monte Carlo integration performs superior than Monte Carlo integration for integrands of bounded variation in the sense of Hardy and Krause [Nie92]. For integrands with unknown discontinuities like the integrand in (2) only pessimistic error bounds are accessible for quasi-Monte Carlo integration [Hla71]. Nevertheless numerical experiments [Kel98a] reveal that even for these functions low discrepancy sampling performs better than random sampling.

3.1 Multiple Importance Sampling for Quasi-Monte Carlo

In order to apply quasi-Monte Carlo integration to bidirectional path tracing the subpath generation has to be done using high dimensional low discrepancy points, where the dimension depends on the length of the subpaths. Due to the transport operator points at the beginning of a subpath affect the integration error more than points at the end of a subpath. In accordance the lower dimensions of low discrepancy points often are better equidistributed than their higher dimensions. Therefore the first four dimensions are used to determine the first point of each subpath, the next four for the first scattering events and so on. This interleaving scheme is similar to [Kel98b], however now

we use the multiple importance sampling estimator (5) with deterministic low discrepancy sampling. In order to avoid aliasing different light subpaths have to be used for the estimation of each pixel functional. This is particularly important for the eye connection techniques $p_{k,k}$ (see also Fig. (3)) and is achieved by using consecutive subsequences of a low discrepancy point sequence instead of a repeated finite point set.

Due to the unbounded variation of the integrand and the deterministic nature of quasi-Monte Carlo, an a-priori error bound by the Koksma-Hlawka inequality as well as an a-posteriori stochastic error estimate is not accessible.

4 Randomized Quasi-Monte Carlo Bidirectional Path Tracing

Randomized quasi-Monte Carlo integration exploits the benefits of low discrepancy sampling and at the same time allows for an efficient error estimate.

From an arbitrary low discrepancy point set $P := \{a_1, a_2, \dots, a_m\} \subset I^s$ we generate r randomized replications $X_j := \{x_{1,j}, x_{2,j}, \dots, x_{m,j}\} \subset I^s$ with $1 \leq j \leq r$ such that

- each replication X_j preserves the low discrepancy properties of P and
- the replications $\{x_{i,1}, x_{i,2}, \dots, x_{i,r}\}$ of each point $a_i \in P$ are independent and uniformly distributed on I^s .

Then the randomized quasi-Monte Carlo estimator with a total of $n = rm$ samples

$$\int_{I^s} f(x) dx \approx \frac{1}{r} \sum_{j=1}^r \frac{1}{m} \sum_{i=1}^m f(x_{i,j}) \quad (8)$$

is unbiased. The expected error is bounded by the square root of the variance σ^2 of the above estimator and can be estimated in an unbiased way using the samples of (8):

$$\sigma^2 = \frac{1}{r(r-1)} \sum_{k=1}^r \left(\frac{1}{m} \sum_{i=1}^m f(x_{i,k}) - \frac{1}{r} \sum_{j=1}^r \frac{1}{m} \sum_{i=1}^m f(x_{i,j}) \right)^2$$

Choosing the number r of replications just large enough to obtain a good variance estimate very little performance of the low discrepancy quadrature is sacrificed and adaptive sampling by error estimation is possible yielding much more efficient rendering algorithms. In [Owe98] Owen presents a compact survey of randomization techniques for quasi-Monte Carlo integration. Except for scrambling, which is beyond the scope of this paper, we investigate their application to the bidirectional path tracing algorithm.

4.1 Cranley-Patterson Rotations

Cranley and Patterson [CP76] suggested the following form of randomization: For a replication they added a random shift to each point $a_i \in P$. Thus we have

$$x_{i,j} = a_i \oplus \xi_j := (a_i + \xi_j) \bmod 1$$

with independent realizations $\xi_j \sim U(I^s)$ for $1 \leq i \leq m$ and $1 \leq j \leq r$. It is straight forward to apply randomized quasi-Monte Carlo integration to bidirectional path tracing using a high dimensional low discrepancy point set with Cranley-Patterson rotations. The assignment of dimensions to the points of the subpaths is the same as used in the quasi-Monte Carlo case (see Sect. 3.1).

4.2 Padded Replications Sampling

Reordering the summation in the estimator in (8) and inserting Cranley-Patterson rotations yields

$$\begin{aligned} \sum_{j=1}^r \sum_{i=1}^m f(x_{i,j}) &= \sum_{i=1}^m \sum_{j=1}^r f(\xi_j \oplus a_i) \\ &\approx \sum_{i=1}^m \int_{I^s} f(x \oplus a_i) dx = \int_{I^s} f(x) dx . \end{aligned}$$

This means that the algorithm is unbiased for any choice of the point set P , which only will affect the variance and therefore the error. If we look at the subpath generation we have to do either area sampling or scattering. Both are two dimensional problems. Thus the idea of padded replications sampling is to use a randomly shifted replicate of the same two dimensional basis pattern for each two dimensional subproblem as illustrated in Fig. 2.

Good Lattice Points. Most low discrepancy constructions are designed to minimize the star-discrepancy in the sense of (t, m, s) -nets or (t, s) -sequences. By randomly shifting a point set P the discrepancy of a replication X_j can be different and especially worse than the original discrepancy [Tuf96], since the (t, m, s) -nets property is not shift invariant. Points P designed to also minimize the shift invariant torus discrepancy [BC87] are suited much better for Cranley-Patterson rotations. Due to their construction good lattice points are better suited for shifting, since their good equidistribution properties almost remain unaffected when being shifted [CP76,SJ94].

5 Latin Supercube Sampling

For the light transport problem the benefits of quasi-Monte Carlo integration diminish in high dimensions [Kel98a]. Latin supercube sampling [Owe97] is a

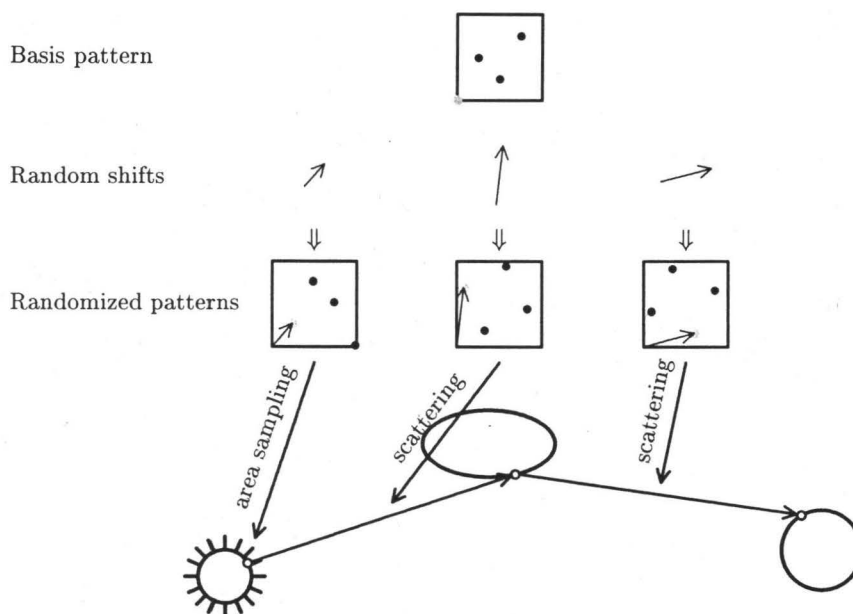


Fig. 2. Subpath generation by padded replications sampling for the example of a light subpath. The basis pattern size is $m = 4$ and the dimension of the padded points is $s = 6$.

method to expand low dimensional samples to high dimensions such adapting to the structure of the transport problem, e.g. low dimensional emission and scattering events. Different from padded replications sampling for Latin supercube sampling the low dimensional point sets are randomly permuted before padding. Suppose that $P_i := \{a_{i,1}, a_{i,2}, \dots, a_{i,n}\} \subset I^d$ for $1 \leq i \leq k = \frac{s}{d}$ are (randomized) quasi-Monte Carlo point sets. Then the Latin supercube samples are

$$x_j := (a_{1,\pi_1(j)}, a_{2,\pi_2(j)}, \dots, a_{k,\pi_k(j)}) \subset I^s$$

for $1 \leq j \leq n$, where the π_i are independent uniform random permutations over $\{1, 2, \dots, n\}$.

In computer graphics Latin supercube sampling is called *uncorrelated sampling*. It already has been applied by [Coo86] (later formalized by [Shi90]) for distribution ray tracing, which is not a consistent algorithm in the sense of (3) since it uses only a subset of the techniques $p_{k,0}$ and $p_{k,1}$, where the end of an eye subpath has to hit a light source or is connected with a point on a light source. However, Cook and Shirley did not use (randomized) quasi-Monte Carlo point sets but stratified random point sets for Latin supercube sampling.

5.1 Latin Supercube Samples from Deterministic Low Discrepancy Points

For bidirectional path tracing Latin supercube sampling allows to pad two dimensional low discrepancy point sets together instead of using high dimensional low discrepancy points. The memory usage for the permutations linearly depends on the number m of the points in the two dimensional point set. Therefore it is recommended to use a small point set. Since this implies that only a small number of different light subpaths can be generated, Latin supercube sampling is only practicable if the eye connection techniques $p_{k,k}$ are not used, otherwise severely disturbing aliasing artifacts will be visible (see Fig. (3)).

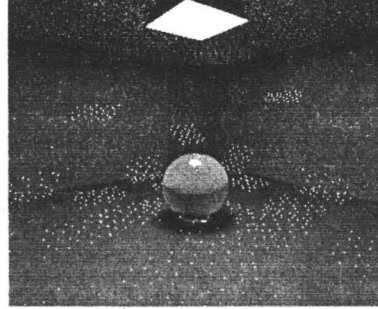


Fig. 3. Aliasing caused by Latin supercube samples from deterministic points with eye connection techniques.

5.2 Latin Supercube Samples from Randomized Low Discrepancy Points

For padded replications sampling the same basis pattern is padded together to form a high dimensional point set P . The resulting correlation between the odd respectively even dimensions can cause an increased variance for a larger number of points in the basis pattern. In order to reduce the correlation Latin supercube sampling can be applied. Numerical experiments show that one initial set of permutations sufficiently decorrelates the padded point set P for the use with the Cranley-Patterson replication scheme.

6 Numerical Experiments

For the numerical experiments we chose the GLASS SPHERE and OFFICE scene as test scenes. Figure 4 shows master images, which have been rendered with the original bidirectional path tracing algorithm using more than a thousand samples per pixel and technique. In our experiments the error of an image is approximated by its L_2 -distance to these master images. Instead of using an absorbing Markov chains for subpath generation we restricted the maximum path length to $k_{\max} = 6$ for the GLASS SPHERE and to $k_{\max} = 3$ for the OFFICE scene.

The difficulties of the GLASS SPHERE scene are the caustic on the floor and the light, which is reflected by the glass sphere onto the ceiling. The OFFICE scene has only diffuse surface properties. Besides the two big luminaries at the

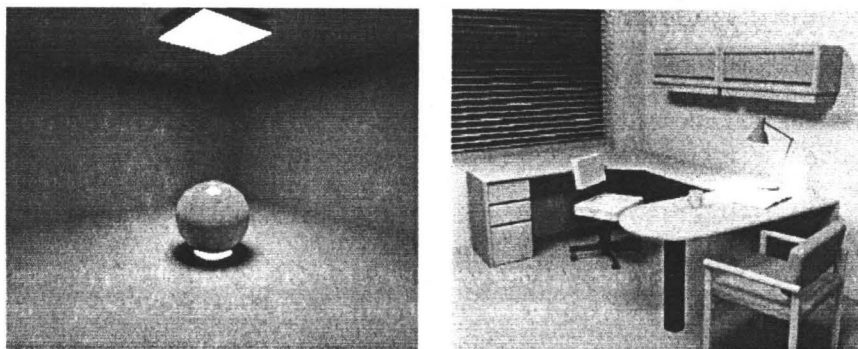


Fig. 4. The GLASS SPHERE and OFFICE scene are used as test scenes.

ceiling the small spherical light source of the table lamp makes the rendering complicated. Since we have no singular surface properties we omit the eye connection techniques $p_{k,k}$, which are only useful in order to render directly seen caustics.

6.1 Blending between Monte Carlo and Quasi-Monte Carlo

The following sampling approaches to the bidirectional path tracing algorithm are compared:

- **Monte Carlo (MC)**
The original bidirectional path tracing algorithm uses pure random sampling. Just for comparison we also implemented a version where we use Latin hypercube sampling.
- **Randomized quasi-Monte Carlo (RQMC)**
For this method we have two possible approaches depending on how the point set P is chosen. The first version (see Sect. 4.1) uses the scrambled Hammersley point set [Fau92]. The second alternative of padded replications sampling (see Sect. 4.2) is based on the two dimensional Hammersley point set. In both approaches we can choose the size m of the point set that is to be replicated.
- **Quasi-Monte Carlo (QMC)**
Here the scrambled Halton sequence [Fau92] is used.

In Fig. 5 convergence graphs are shown. As expected the convergence rates for the Monte Carlo and randomized quasi-Monte Carlo versions are $\mathcal{O}(n^{-1/2})$, where n denotes the total number of samples per technique and pixel. A slightly improved rate of $\mathcal{O}(n^{-1/2-\alpha})$ can be observed for the quasi-Monte Carlo approach, where $\alpha \in [0, \frac{1}{2}]$ decreases with the maximum path length k_{\max} used in the simulation.

For a more detailed comparison we measured the number of samples required to achieve a given error in relation to the number needed by the

original bidirectional path tracing algorithm, i.e. the pure Monte Carlo algorithm. The results are shown in Fig. 6. Far more than half of the expensive samples can be saved by the quasi-Monte Carlo version. The randomized quasi-Monte Carlo approaches form a smooth transition between the pure random and the deterministic algorithm. With an increasing size m of the point set P the error decreases due to the better equidistribution of the samples. It is an interesting result that for bidirectional path tracing padded replications sampling performs at least as good as a high dimensional low discrepancy point set.

6.2 Latin Supercube Sampling (LSS)

- **By Deterministic Low Discrepancy Points.**

Since the eye connection techniques are not used to render the OFFICE scene, Latin supercube sampling can be applied. For padding the two dimensional Hammersley point set was chosen. In comparison to the pure Monte Carlo algorithm only 35% of the samples are needed to achieve the same error. Thus it performs similar to the purely deterministic quasi-Monte Carlo approach (37%, see Fig. (6)).

- **By Randomized Low Discrepancy Points.**

As proposed in Sect. (5.2) Latin supercube sampling can reduce the correlation between the dimensions of the points used by padded replications sampling. The problem of that correlation is slightly visible in Fig. (6) for the OFFICE scene when increasing the basis pattern size m from 16 (42%) to 32 (45%).

In Fig. (7) padded replications sampling with and without Latin supercube sampling is compared, where we padded replications of the Fibonacci lattice points [SJ94]. Note that the permutation is only applied once before creating the randomized replications by Cranley-Patterson

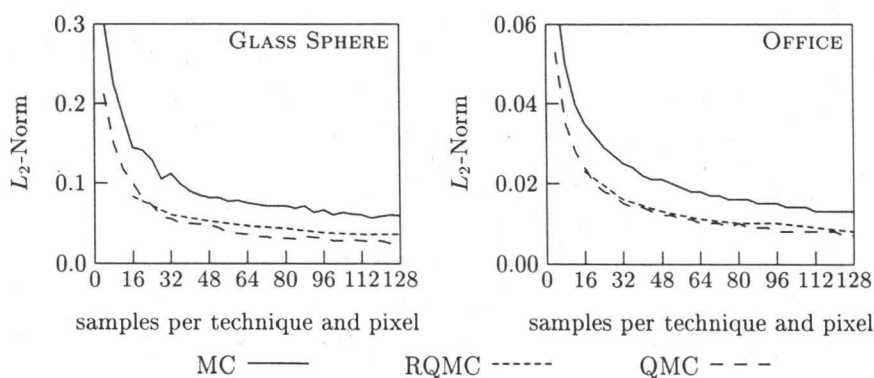


Fig. 5. Convergence graphs for MC, RQMC ($m = 16$), and QMC.

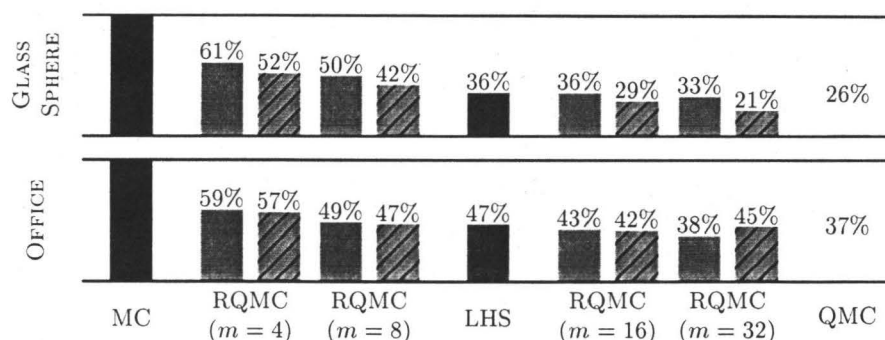


Fig. 6. Number of samples needed to achieve a given error in relation to MC. Padded replications sampling (left bars of RQMC) performs at least as good as the straight forward approach (right bars of RQMC).

rotations (see Sect. (5.2)). The reduced correlation results in a better performance when using bigger basis pattern sizes m . In computer graphics, however, $rm = n \in \{8, \dots, 128\}$ so that the effect of decorrelation by Latin supercube sampling is hardly perceivable.

6.3 Visual Comparison

For a visual comparison of images we rendered the OFFICE scene with the original bidirectional path tracing algorithm and with the padded replications sampling (Hammersley, no Latin supercube sampling) approach using 16 samples per technique and pixel. Since the padded replications sampling version needs less pseudo random numbers its rendering time was about 12% shorter. Figure 8 shows two close-ups of the images. The reduced error results in a less noisy image. Even in only indirectly illuminated regions (right column) there is less noise.

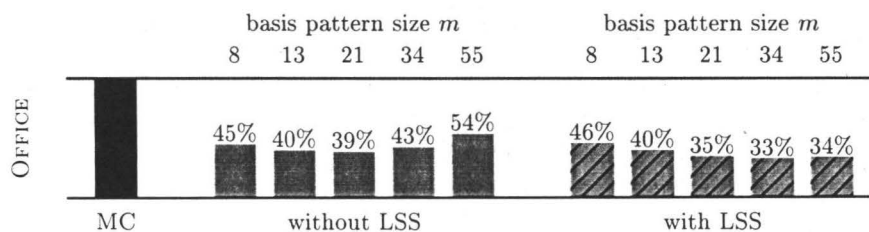


Fig. 7. Using Latin supercube samples as input for Cranley-Patterson replication reduces the effect of correlation arose by padded replications sampling. For this experiment Fibonacci lattice points have been used as basis pattern.

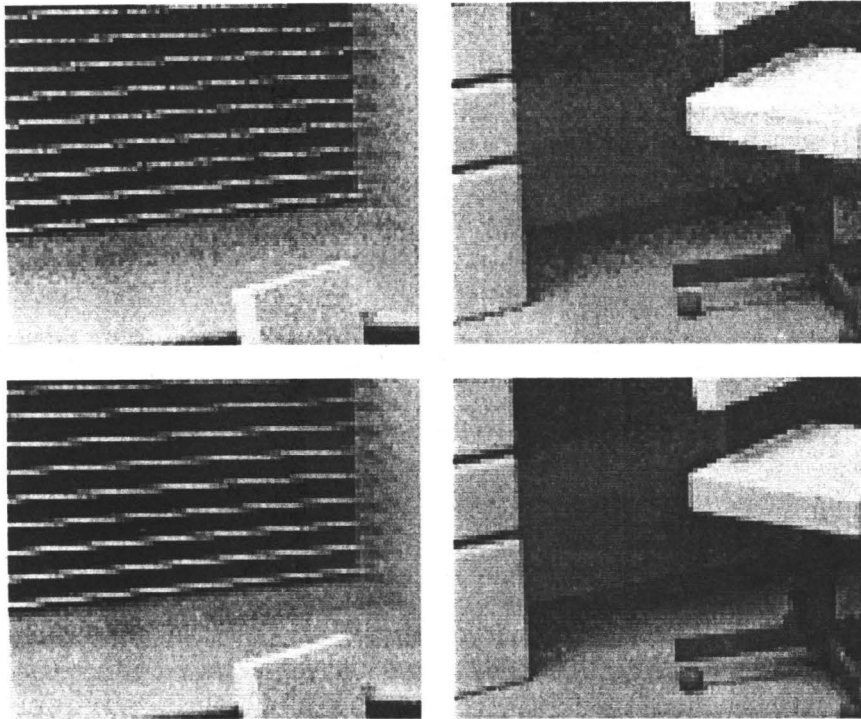


Fig. 8. Image comparison. The close-ups in the upper row were rendered with pure Monte Carlo bidirectional path tracing and the close-ups in the lower row were rendered by the padded replications sampling (Hammersley, no Latin supercube sampling) approach.

7 Conclusion

We investigated several sampling approaches to bidirectional path tracing based on Monte Carlo extensions of the quasi-Monte Carlo method. Therefore we first transferred multiple importance sampling to quasi-Monte Carlo integration yielding a much more efficient algorithm but losing the possibility to estimate the error. Bidirectional path tracing by randomized quasi-Monte Carlo integration is almost as efficient as deterministic low discrepancy bidirectional path tracing, however the error easily can be estimated.

In order to avoid the generation of high dimensional low discrepancy points padded replications sampling has been introduced. The resulting correlation between the dimensions of the points has been reduced by Latin supercube sampling, such that even large basis pattern sizes can be used without loss of efficiency. Padded replications sampling perfectly fits the structure of the light transport problem and its application to bidirectional path tracing is simple to implement.

The efficient application of Owen's scrambling techniques as well as adaptive sampling to bidirectional path tracing is subject of our future research.

Acknowledgement

The authors would like to thank Fred Hickernell for his comments during the conference.

References

- [BC87] J. Beck and W. Chen, *Irregularities of Distribution*, Cambridge University Press, 1987.
- [Coo86] R. Cook, *Stochastic Sampling in Computer Graphics*, ACM Transactions on Graphics **5** (1986), no. 1, 51–72.
- [CP76] R. Cranley and T. Patterson, *Randomization of Number Theoretic Methods for Multiple Integration*, SIAM Journal on Numerical Analysis (1976), 904–914.
- [Fau92] H. Faure, *Good Permutations for Extreme Discrepancy*, J. Number Theory (1992), no. 42, 47–56.
- [Hla71] E. Hlawka, *Discrepancy and Riemann Integration*, Studies in Pure Mathematics (L. Mirsky, ed.), Academic Press, New York, 1971, pp. 121–129.
- [Kel98a] A. Keller, *Quasi-Monte Carlo Methods for Photorealistic Image Synthesis*, Ph.D. thesis, Shaker, Aachen, 1998.
- [Kel98b] ———, *The Quasi-Random Walk*, Monte Carlo and Quasi-Monte Carlo Methods in Scientific Computing 1996 (H. Niederreiter, P. Hellekalek, G. Larcher, and P. Zinterhof, eds.), vol. 127, Springer, 1998, pp. 277–291.
- [KW86] M. Kalos and P. Whitlock, *Monte Carlo Methods, Volume I: Basics*, John Wiley & Sons, New York, 1986.
- [LW93] E. Lafortune and Y. Willems, *Bidirectional Path Tracing*, Proc. 3rd International Conference on Computational Graphics and Visualization Techniques (Compugraphics), 1993, pp. 145–153.
- [Nie92] H. Niederreiter, *Random Number Generation and Quasi-Monte Carlo Methods*, SIAM, Pennsylvania, 1992.
- [Owe97] A. Owen, *Latin Supercube Sampling for Very High Dimensional Simulations*, Tech. report, Stanford University, 1997.
- [Owe98] ———, *Monte Carlo Extension of Quasi-Monte Carlo*, Winter Simulation Conference, IEEE Press, 1998, pp. 571–577.
- [OZ99] A. Owen and Y. Zhou, *Safe and Effective Importance Sampling*, Tech. report, Stanford University, Goldman-Sachs, 1999.
- [Shi90] P. Shirley, *Physically Based Lighting Calculations for Computer Graphics*, Ph.D. thesis, University of Illinois, Urbana-Champaign, 1990.
- [SJ94] I. Sloan and S. Joe, *Lattice Methods for Multiple Integration*, Clarendon Press, Oxford, 1994.
- [Sob94] I. Sobol, *A Primer for the Monte Carlo Method*, CRC Press, 1994.
- [Tuf96] B. Tuffin, *On the Use of Low Discrepancy Sequences in Monte Carlo Methods*, Monte Carlo Methods and Applications **2** (1996), no. 4, 295–320.
- [VG94] E. Veach and L. Guibas, *Bidirectional Estimators for Light Transport*, Proc. 5th Eurographics Workshop on Rendering (Darmstadt, Germany), June 1994, pp. 147–161.